

# A numerical scheme for tracking cyclone centres from digital data

## Part I: development and operation of the scheme

Ross J. Murray and Ian Simmonds

Department of Meteorology, University of Melbourne, Australia

(Manuscript received November 1990; revised March 1991)

**An automated scheme for finding and tracking cyclones from numerical analyses is described and its performance is discussed. It embodies several computational features not previously applied in this context and circumvents much of the labour that has hindered this work in the past. The scheme has been developed and tested with both observed and model-generated data, and particularly with a view to its suitability for studying the behaviour of southern hemisphere extratropical cyclones.**

### Introduction

Weather patterns in extratropical latitudes are largely controlled by the passage of migratory cyclonic systems and their associated fronts. The importance of understanding the behaviour of these systems has long been recognised and over the past forty years many workers have plotted tracks of these storms with the object of describing and explaining their development, movement and distribution.

Studies based in the northern hemisphere (NH) have been greatly facilitated by the availability of analyses going back to the turn of the century and, since 1958, by the publication of plotted cyclone paths in the *Mariners' Weather Log* and *Climatological Data, National Summary*. No such resource exists for the southern hemisphere (SH), and attempts to gain an understanding of cyclonic behaviour on a hemispheric scale were greatly impeded by poor data coverage over the southern oceans until the 1970s. Nevertheless, the publication of hemispheric charts prepared during the International Geophysical Year (IGY) programme of 1957–58 did make possible the landmark contribution of Taljaard (1967) during this period.

With the advent of satellite imagery and the improved analyses that became available during the 1970s, a number of workers, including Streten and Troup (1973), Carleton (1979), Le Marshall and Kelly (1981) and Kep (1984), compiled cyclone statistics for the SH for various periods covering a number of years. The exercise of recording positions and following them from day to day has proven to be a very tedious and time-consuming operation. Moreover, where operational charts have been used (e.g. by Kep), inconsistencies may have arisen in the identification of low centres by analysts from day to day, and in the association of successive daily positions of systems.

To overcome these drawbacks, an automated scheme has been devised to perform the work using digital mean sea level (MSL) pressure data. This evolved from a simpler version developed by Rice (1982) for use with SH analyses. In the present scheme, which is described in the following section, the pressure fields are fitted by analytic functions. Low pressure centres are located, their paths are tracked from birth to decay, and various statistics of their distribution and movement are analysed. All three stages of the scheme are performed without intervention, once a number of governing constants have been decided upon, thus allowing objective comparisons to be made

*Corresponding author address:* Dr I. Simmonds, Department of Meteorology, University of Melbourne, Parkville, Victoria 3052, Australia.

between the cyclone statistics obtained from different data sets. This not only renders it suitable for a reworking of historical analyses but also makes it especially appropriate for the analysis of model-generated data.

The speed of a computer-based scheme has permitted a very satisfactory solution to the problem of applying differential methods for minimum determination. The procedure that has been arrived at enables both deep and shallow depressions to be detected and accurately located, thereby assisting the tracking of cyclones which occurs in the next stage of the scheme. The association of successive daily positions is based upon the estimated displacements of systems between one analysis period and the next. Because these are computed in an essentially statistical manner and without physically based modelling of cyclone movements, the accuracy of the individual storm tracks cannot always be assured. The performance of the tracking program and the possibility of bias to the cyclone statistics are discussed later in this paper. A more extensive analysis of track statistics than heretofore available has been made possible, and the opportunity has been taken to take a new approach to grid sampling and scaling.

Both observed and model pressure fields were employed in the development of the scheme. The former were taken from the twice-daily World Meteorological Centre (WMC) numerical analyses available from the Australian Bureau of Meteorology and the latter from the 15 and 21-wave versions of the University of Melbourne general circulation model (GCM) (Simmonds 1985). The 21-wave GCM data proved to be the most suitable for this purpose, and most of the refinements to the scheme were made to suit these data.

The scheme has been used to investigate the synoptic climatology of the 21-wave simulations for January and July: the results of this study will be given in Part II (Murray and Simmonds 1991).

## Description of the scheme

### Fitting the pressure field

In order to facilitate the location of low centres from digital analyses, it was considered desirable to have pressures specified on a conformal or near-conformal projection. The WMC analyses are archived on a  $47 \times 47$  SH polar stereographic (PS) grid which has this property. For computational convenience and because it has a map factor which can be taken to be locally constant, the PS grid is used in all three stages; however, this is not an immutable feature of the scheme.

At the resolution of the grid, which is characteristically of the order of 500 km, the grid spacing is comparable with the radius of many of the

smaller synoptic depressions identified on operational charts. It was therefore found advantageous to model the form of the pressure surface between grid-points analytically, using a two-dimensional polynomial representation; this was found to be most efficiently achieved by fitting a bicubic spline function to the entire array. Pressures are interpolated by applying a Taylor's expansion to the pressure and its 15 derivatives using the equation:

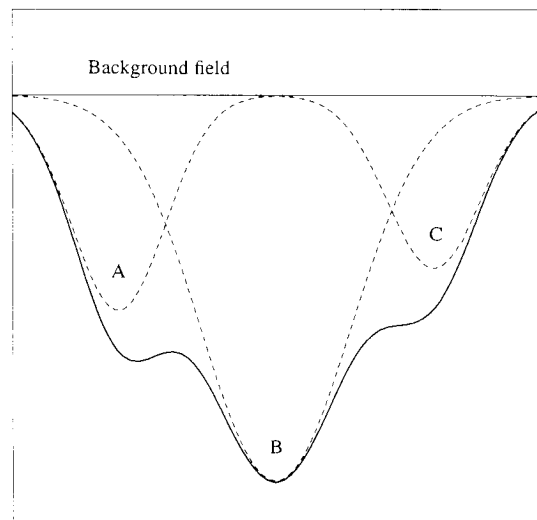
$$p(x_i + \delta x, y_j + \delta y) = \sum_{m=0}^3 \sum_{n=0}^3 p_{x^m y^n}(x_i, y_j) \delta x^m \delta y^n, \quad \dots 1$$

where

$$p_{x^m y^n} = \frac{\partial p^{m+n}}{\partial x^m \partial y^n}. \quad \dots 2$$

It is instructive to think of the instantaneous pressure field as being built up from the superposition of a number of bell-shaped functions of varying amplitudes upon some constant or climatic average field, as suggested by Williamson (1981). As will be appreciated from Fig. 1, a medium-sized cyclonic disturbance placed in the vicinity of a larger one may generate only a small shallow region of closed isobars (depression A) or possibly none at all (depression C), yet the extent of the disturbance may be inferred from the concave form of the pressure surface to some distance from the centre.

Fig. 1 A hypothetical pressure field built up from the superposition of three archetypal cyclonic disturbances (A, B and C) upon a uniform field.



In the case of the GCM data, the atmospheric variables are defined globally in the spectral representation of the model output and MSL pressures could, in principle, be found at any point from summations of the local values of the spherical harmonics: in practice, however, the evaluation of pressures at large numbers of grid-points and intermediate points by this means would be a very inefficient process. It has therefore been necessary to synthesise pressures on a (non-conformal) latitude-longitude grid and to interpolate these data on a PS grid. MSL pressure fields were extracted from the 15 and 21-wave daily model histories on  $4.4 \times 7.5^\circ$  and  $3.3 \times 5.6^\circ$  grids and interpolated (also by bicubic spline interpolation) onto  $47 \times 47$  and  $61 \times 61$  PS grids, having polar grid spacings of 5.0 and 3.8 deg. lat., respectively.

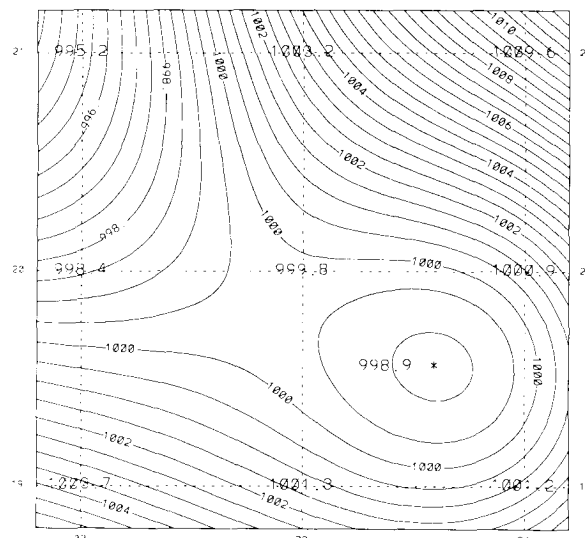
#### Finding the positions of low centres

The method usually employed for finding lows from gridded data involves a comparison of pressures at neighbouring points. A cyclone is deemed to exist at any point at which the pressure is lower than at any of a small number of grid-points (4 or 8) surrounding it. This method has been employed in recent studies by Lambert (1988) and Bell and Bosart (1989). It is also used in graphics utilities for plotting highs and lows on contour maps: in this type of application the minimisation may be taken over a larger number of points to prevent clutter.

The above technique has the disadvantage of failing to identify some of the systems of meteorological interest when the grid spacing is of the same order as their expected dimensions. As mentioned before, a simple comparison of grid-point pressures takes no account of the likely variation of pressures between grid-points. While still only an approximation to the unknown form of the pressure surface between grid-points, it is nevertheless believed that a higher order fit, such as the one described earlier, is a better approximation than the essentially linear representation of a grid-based method. (This comment has particular validity in regard to pressures interpolated from spectrally truncated data.) It has frequently been found possible for the bicubic fit to synthesise a small depression in the absence of a nearby minimum grid-point pressure: an example of this is illustrated in Fig. 2. Another difficulty is that when the grid spacing is not small compared to the expected displacement between analysis times, the approximation of cyclone positions by grid-points tends to result in a jerky checkerboard type of motion that complicates tracking and almost rules out useful calculations of cyclone velocity.

The problems referred to may be alleviated by approximating the pressure surface by smoothly varying functions. An obvious way of using them would be to interpolate the data onto a finer grid

Fig. 2 Isobars interpolated from grid-point pressures, nine of which appear in the plot, and the pressure minimum (asterisk) located by the final version of the program.



and then carry out the comparison of pressures on the new grid. This has been done by Grotjahn (1990) to construct small grids for matching features in analysed and forecast fields. The method we have employed is rather different from this and allows cyclones to occupy a continuous range of positions between grid-points. For this purpose the finding procedure was modified to a two-stage process.

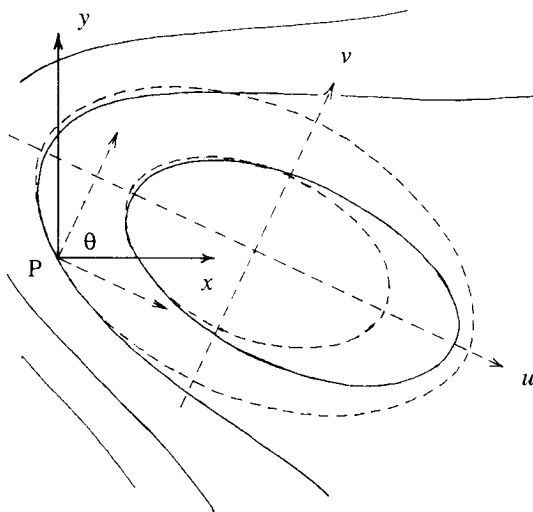
The array is first of all scanned for the sites of 'possible' lows by comparing the values at neighbouring grid-points. To allow for the possibility that a shallow depression may not be detected by a local minimisation of grid-point values, a less restrictive scanning procedure has been implemented. This procedure seeks grid-points at which the Laplacian of the pressure,

$$\nabla^2 p(x_i, y_j) = p_{xx} + p_{yy}, \quad \dots 3$$

shall be greater than at any of the eight surrounding points and greater than a prescribed positive value. The scanning technique resembles the method used by Le Treut and Kalnay (1990), who identified lows with grid-point pressures at least 4 hPa lower than the mean over the closest 20 grid-points surrounding it.

From each of these points the finding program searches for a local minimum pressure. This is approached in an iterative fashion by using the (interpolated) first and second space derivatives of the pressure at one point to define an ellipsoid, whose centre becomes the next point in the iteration (Fig. 3). The orientation,  $\theta$ , of the axes is given by

**Fig. 3** An example of a pressure pattern (solid lines) and the contours and axes ( $u$  and  $v$ ) of the ellipsoid of best fit (broken lines) defined by the derivatives at the point P.



$$\tan 2\theta = \frac{2p_{xy}}{p_{xx} - p_{yy}} \quad \dots 4$$

and the second derivatives in the axial directions by

$$p_{uu} = \frac{p_{xx} + p_{yy}}{2} - \sqrt{\left(\frac{p_{xx} - p_{yy}}{2}\right)^2 + p_{xy}^2} \quad \dots 5$$

$$p_{vv} = \frac{p_{xx} + p_{yy}}{2} + \sqrt{\left(\frac{p_{xx} - p_{yy}}{2}\right)^2 + p_{xy}^2} \quad \dots 6$$

where  $u$  and  $v$  are coordinates taken from the centre of the putative ellipsoid along the major and minor axes, respectively. The iterative technique is a two-dimensional extension of the Newton-Raphson algorithm, which can be applied independently to the  $u$  and  $v$  coordinates, viz.

$$u_{(n+1)} = u_{(n)} - \frac{p_u(u_{(n)})}{p_{uu}(u_{(n)})} \quad \dots 7$$

$$v_{(n+1)} = v_{(n)} - \frac{p_v(v_{(n)})}{p_{vv}(v_{(n)})} \quad \dots 8$$

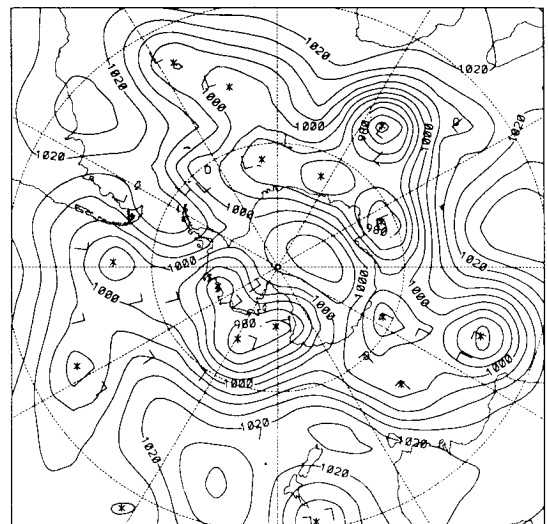
Provided that a true minimum (i.e. a point at which the minimum second derivative  $p_{uu} > 0$  and  $p_u = p_v = 0$ ) can be found within a specified radius of search, convergence to within 0.001 grid units of the minimum normally occurs within three or four iterations. The numbers and positions of centres identified by the finding program have been in good agreement with those inferred from the contoured numerical analyses. The position and central pressure of one such low is shown along with the contours of the interpolated pressure in Fig. 2.

**Incorporation of open depressions**

The scheme was first tested with twice-daily data from WMC analyses for July 1977. An average of 12 mid-latitude cyclones was found by the original version of the finding program at each synoptic time, but these represented fewer than half of the lows that were identified manually on the corresponding operational charts by analysts at the Bureau of Meteorology (normally about 30) (Fig. 4). On the other hand, there were often one or two lows north of the subtropical ridge found by the program but not identified on operational charts.

By its nature, the low-finding procedure is able to discover a depression, however shallow, provided that a true minimum pressure exists at some point within it: it is not restricted by, for example, the need to find a closed isobar at some finite contour interval. At low latitudes, where background pressure gradients are weak, this ability tends to result in the analysis of many insignificant depressions of no meteorological interest. In the mid-latitude zone the problem is the reverse. Apparently some of the less prominent systems identified by analysts in data-sparse areas are not always revealed as pressure minima in the numerical analyses by the insertion of pseudo-observations based on the interpretation of cloud imagery (Guymer 1978, 1986) on a finite resolution grid.

**Fig. 4** Pressure pattern and cyclone centres analysed by the scheme (south of 15°S) from the 1100 UTC 19.7.1977 numerical analysis. The asterisks indicate closed depressions and the circles open depressions. The 'L's mark the positions of lows appearing on the manual analysis for 1200 UTC on the same date. There are three open depressions (at 40°S 50°E, 60°S 135°E, and 60°S 35°W), each lying close to a manually analysed low.



The two types of disparity are linked by a unifying consideration. Comparison of the corresponding analyses indicated that in most cases a low marked on the operational chart can be identified with a significant cyclonic distortion of the pressure pattern on the contoured numerical analysis, whether or not associated with a region of closed isobars. Subtropical pressure minima not recognised on the operational charts, however, did not possess this property. The type of feature referred to is always associated with a marked concavity in the pressure surface, i.e. a maximum of  $\nabla^2 p$ , and hence a maximum of relative cyclonic geostrophic vorticity ( $\xi$ ), since

$$\xi \approx \frac{1}{\rho f} \nabla^2 p, \quad \dots 9$$

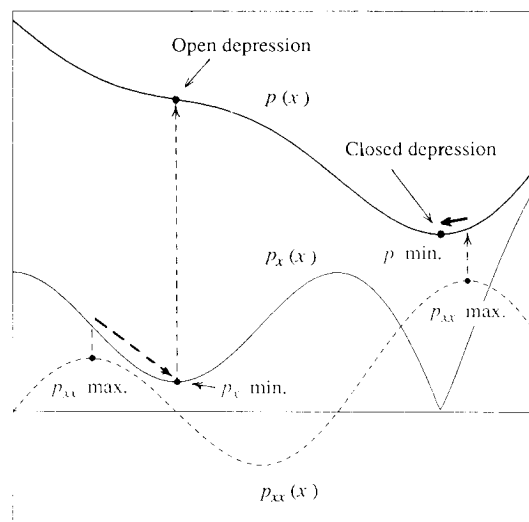
where  $\rho$  is the air density and  $f$  the Coriolis parameter. It is concluded that, at least as far as synoptic-scale digital analyses are concerned, the existence of a mid-latitude depression is better represented by a pronounced cyclonic vorticity maximum than by a pressure minimum.

It is convenient to refer to depressions as 'closed' or 'open' according to whether they possess regions of closed isobars or not. The centre of a closed system is unequivocally identified with its point of minimum pressure; this is normally found within one grid space of the  $\nabla^2 p$  maximum, depending on the degree of symmetry of the cyclone. In the case of an open depression no such point exists, but it was decided that a suitable analogue for it would be the inflexion in the pressure surface, i.e. the point of minimum pressure gradient, which is nearly always associated with a concavity in the pressure field. The point of inflexion could be taken to indicate the most likely location of a closed system below the limit of resolution imposed by the grid or by the analysis.

As before, the low-finding procedure scans the array for grid-points at which  $\nabla^2 p$  is maximised and each such position is taken as the starting point in the search for a pressure minimum (a closed depression). If a closed depression cannot be found within a suitable radius, the program, starting from the same grid-point, will seek an open depression by attempting to minimise the magnitude of the pressure gradient. A one-dimensional illustration of this is given in Fig. 5. It will be seen that the absolute pressure gradient at the centre of a closed low, although zero, is not a true minimum and does not admit of discovery by differential means.

The low is then checked for having the character of a mid-latitude storm. The method that was found to give good discrimination is one that requires a minimum average value of  $\nabla^2 p$  over a specified radius of the cyclone centre. (An effective minimum value of  $0.4 \text{ hPa}/(\text{deg. lat.})^2$  over a radius of 4 deg. lat. was used for both open and closed systems with 21-wave data.) The im-

Fig. 5 A cross-section of pressure and its derivatives showing how maxima of  $p_{xx}$  (or  $\nabla^2 p$  in two dimensions) may be used as starting points in the search for both open and closed depressions. A low centre will normally lie fairly close to its associated  $\nabla^2 p$  maximum, but will not be coincident with it unless the depression is exactly symmetrical. To show the principle of this,  $\nabla^2 p$  is represented here as a continuous function: in practice it is sufficient to maximise it from grid-point values.



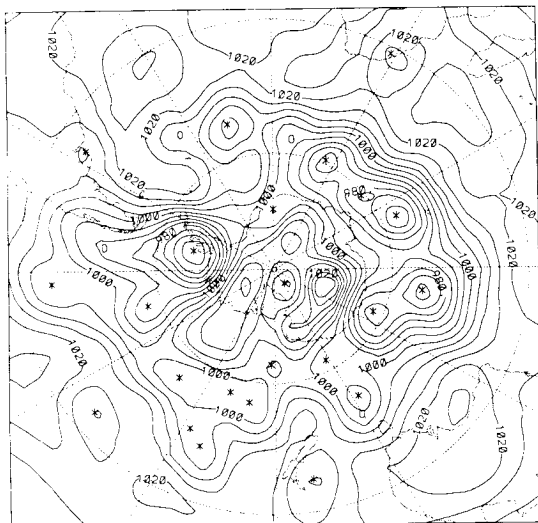
sition of this 'concavity criterion' succeeded in disqualifying most of the closed lows in regions of slack pressure gradients while retaining open depressions marked by a significant distortion of otherwise closely spaced isobars. Other criteria, such as the stipulation of a minimum central pressure or a minimum range of closed contours, were ruled out as being too arbitrary or not in keeping with the intended purpose of the test.

An average of three to four open depressions was found in each numerical analysis. The correspondence of three such features with lows appearing in the manual analysis may be seen in Fig. 4. With the GCM cyclones a similar comparison was, of course, not possible but a subjective assessment indicated the need for including open depressions and applying a concavity criterion to these data too. The numbers of cyclones in the 15-wave model data fields were similar to those found with the WMC numerical analyses, but the 21-wave model generated rather more lows (an average of 15 closed and six open depressions) from each field when a suitable grid resolution was used (Fig. 6). Apparently the higher wave numbers are important for the delineation of synoptic features in the pressure field.

#### Tracking the lows

In the second stage of the scheme the path of each system is tracked from the time of its first appear-

Fig. 6 Isobars and low centres on one day of the 21-wave July simulation. Asterisks mark closed depressions and circles open depressions.



ance to its dissipation. The accumulation of cyclone life histories allows the compilation of statistics on the evolution and movement of storms as well as those of their distribution.

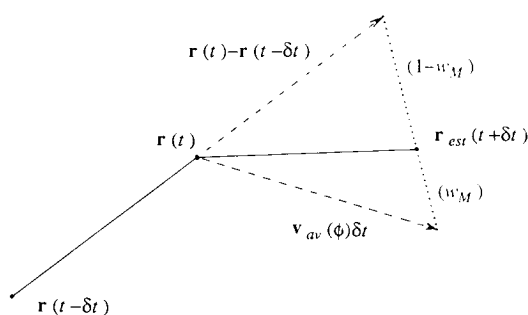
The construction of trajectories could be achieved by searching for a centre within a selected radius of each cyclone position recorded at the previous analysis time. The difficulty with this method is that in a 24-hour period cyclone centres often travel distances which are of the same order as their separations, so one is not always sure where each cyclone has gone during this period. To make the appropriate decisions a procedure was devised which makes an estimate of the new position of each system, calculates the probability of associations between the predicted and realised positions, and finds the matching of these associations with the highest overall probability.

The first of these steps uses climatological cyclone velocity statistics and the previous movement of the system itself to predict a 'most likely' new position and pressure for each cyclone. The position ( $\mathbf{r}$ ) estimated for one time interval ( $\delta t$ ) after the current time ( $t$ ) is obtained by taking a weighted average of the displacement based on the assumed climatological average cyclone velocity,  $\mathbf{v}_{av}(\phi)$ , for the latitude,  $\phi$ , viz.,

$$\mathbf{r}_{est}(t + \delta t) = \mathbf{r}(t) + w_M\{\mathbf{r}(t) - \mathbf{r}(t - \delta t)\} + (1 - w_M)\mathbf{v}_{av}(\phi)\delta t + \mathbf{r}_K \quad \dots 10$$

(vide Fig. 7).  $\mathbf{r}_K$  is a small magnitude term (depending on the cyclone trajectory) included to replicate the acceleration implied by the climatological average cyclone velocities on the PS pro-

Fig. 7 Prediction of a new cyclone position ( $\mathbf{r}_{est}(t + \delta t)$ ) based on weightings  $w_M$  of the previous displacement,  $\mathbf{r}(t) - \mathbf{r}(t - \delta t)$ , and  $(1 - w_M)$  of the displacement based on mean cyclone velocities,  $\mathbf{v}_{av}(\phi)\delta t$ .



jection. No correction is made to allow for the curvature of the great circles or for local changes in the map factor. A central pressure is also estimated for the cyclone based on a weighted combination of persistence and its previous tendency,

$$p_{est}(t + \delta t) = p(t) + w_p[p(t) - p(t - \delta t)] \quad \dots 11$$

The weighting factors quantify the 'memory' of past motion and pressure tendency incorporated in the prediction. There is no reason to suppose that a 50-50 weighting would necessarily be appropriate. For short time intervals a choice of  $w_M$  and  $w_p$  close to or equal to unity would be in order: for long intervals one would select values closer to zero. (Assuming a constant time step and an exponential decay of velocity toward the climatological value with time, a variation with time interval,  $\delta t$ , of the form

$$w(\delta t) = w(\delta t_0)\delta t/\delta t_0 \quad \dots 12$$

would be expected.) On the basis of trials of the scheme, described later, weighting factors,  $w_M = 0.36$  and  $w_p = 0.3$ , were found suitable for use with daily July data: these values imply a relatively low memory of past motion and pressure tendency.

In the next stage of the tracking the probabilities of associations between predicted positions and actual positions at the new analysis period are calculated. Each pair of predicted ( $m$ ) and new ( $n$ ) positions separated by a distance  $r_{mn} < r_c$  is assigned a probability based upon a decreasing function of their separation and central pressure differences. This is done by including a component of pressure differential in the 'radius'.

$$r'_{mn} = \sqrt{r_{mn}^2 + (\delta p_{mn}/k_{rp})^2}, \quad \dots 13$$

where  $k_{rp}$  is an adjustable constant. The problem is then to find the combination of mutually exclusive associations for which the product of the probabilities is maximum.

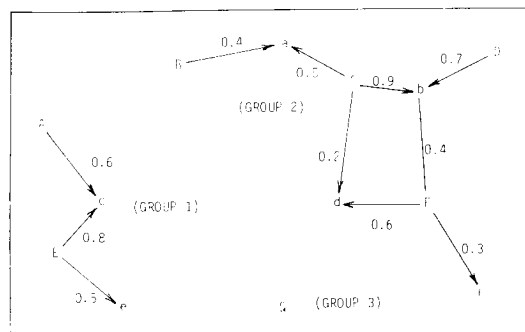
The function,  $\exp((P_{\max})_{mn} - r'_{mn}{}^2/r_c^2)$ , was selected as having the required behaviour, the value of  $P_{\max}$  being adjusted to favour certain cyclone associations. Normally  $P_{\max} = 1$ , but a smaller value of  $P_{\max}$  is employed for associations which include newly formed systems ( $P_{\text{new}}$ ), open depressions ( $P_{\text{open}}$ ), or both ( $P_{\text{new}} \times P_{\text{open}}$ ) in order to inhibit their inclusion in the tracks. Values of  $k_{rp} = 1.4$  hPa/deg. lat.,  $r_c = 12.5$  deg. lat.,  $P_{\text{new}} = 0.75$ , and  $P_{\text{open}} = 0.6$  have been used with 21-wave data.

In practice, the most probable combination of associations is found by maximising the sum of the logarithms of the probabilities, i.e. the sum of the functions.

$$P_{mn} = (P_{\max})_{mn} - \frac{r'_{mn}{}^2}{r_c^2} \quad (r'_{mn} < r_c \sqrt{(P_{\max})_{mn}}) \dots 14$$

This maximisation is achieved by sorting the predicted-new cyclone associations into groups (Fig. 8) and determining the ensemble of matched pairs in each group with the highest overall probability. Histories of the consecutive positions and pressures of each current system are thereby extended by one period, while those which are not paired up in this process are deemed to have been born or to have decayed.

Fig. 8 Grouping of predicted (capitals) and new (small letters) cyclone positions. Values of  $P_{mn}$  are given for possible matchings (arrows) of predicted (upper case) and new (lower case) positions. In each group the combination of associations with the greatest  $\Sigma P_{mn}$  is selected. In group 1 there are two possible matches, Ac.Ee ( $\Sigma P_{mn} = 0.6 + 0.5 = 1.1$ ) and Ec ( $\Sigma P_{mn} = 0.8$ ). The former set has the highest probability in the group and is therefore selected. The resulting matches for group 2 are Ba,Cb,Fd ( $\Sigma P_{mn} = 1.9$ ). After deciding these matchings we see that cyclones D and G are defunct and f is new.



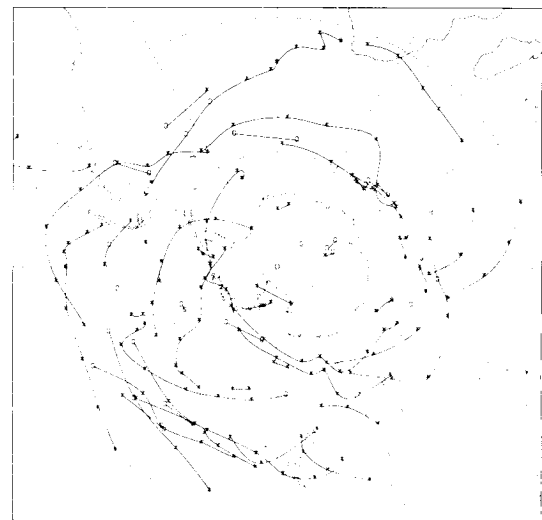
**Analysis of cyclone track statistics**

An analysis program has been written for obtaining the average values of a number of quantities from the accumulated track histories. The ability to retrieve these data easily has allowed a variety of statistics to be computed. These include those of the spatial density, flux, velocity, central pressure, and pressure tendency of cyclones, and the frequencies of cyclogenesis and cyclolysis.

Statistical summations are compiled from cyclone properties taken at regular time intervals. Since cyclones may move two or more grid spaces in the course of a day, a representative sampling of the data for calculating zonal and regional cyclone statistics is effected by fitting cubic splines to the position coordinates and central pressures of systems, and by interpolating the values of these quantities and their time derivatives at intermediate times. A frequency of five sampled positions/day (i.e. one recorded position and four interpolated positions) has been found adequate. The interpolated positions and pressures are also used to aid the visualisation and discrimination of tracks and time series. The paths of 21-wave cyclones tracked over a ten-day period are shown in Fig. 9.

The lifespan of a system is reckoned to be the interval between the first and last analysis time recorded in the track history (cyclogenesis and cyclolysis). A minimum lifespan of at least one analysis period (i.e. 24 hours normally) is imposed

Fig. 9 Tracks of cyclones for ten days from consecutive positions at 24-hour intervals (21-wave July simulation). Curves connect the positions of systems surviving 24 hours or more. Asterisks mark closed depressions and circles open depressions.



in order to exclude ephemeral systems from the averaging and to enable the calculation of time derivatives (velocity and pressure tendency).

Regional cyclone statistics are compiled at (PS) grid-points after the application of a smoothing procedure, applied in such a way as to conserve the total numbers of systems. Zonal averages are computed from summations over chosen latitude intervals (normally 5°) and no smoothing is applied.

In calculating frequencies of cyclonic events, it is usual to normalise the resulting totals for averaging period and grid size. Thus, for instance, frequencies of cyclogenesis and cyclolysis are obtained from counts made at the first and last analysed position of each track, respectively, and are normalised for time and area. In calculating frequencies of cyclone occurrence, the applicability of area normalisation has been disputed (Hayden 1981) and some workers have preferred to allow totals to stand as raw numbers. The matter has been confused by the fact that cyclone occurrence may be reckoned either as a spatial density or as a flux. Writers in the past have employed a variety of sampling and normalisation methods and have not always made it clear which of these two essentially different measures was intended.

*Cyclone density* is the number of cyclones/unit area found in a particular region and is calculated by summing contributions from all sampled positions (recorded or interpolated along the tracks) and normalising for area and the number of sampling times. Taljaard (1967) and a number of later authors have calculated densities of SH cyclones in units of 'cyclones/ $5 \times 10^\circ$  normalised block/4 month season'. The reference to time is misleading. The quantity may be considered a measure of the proportion of the time that a point will be under cyclonic influence but is independent of the units in which time is measured.

*Track flux* refers to the number of systems passing within unit distance of some point per unit time. For some purposes, it has been found preferable to calculate the net vector averaged flux of eastward (or northward) cyclone crossings/unit meridian (or parallel)/unit time, or its scalar magnitude. Net fluxes tend to eliminate the sometimes unwanted contributions of quasi-stationary systems.

The method of calculating cyclone frequencies (essentially track fluxes) that has been used in many NH studies (Klein 1957; Reitan 1974; Zishka and Smith 1980; and Whittaker and Horn 1982) has been to count each system only once in any grid square. This procedure suffers from the defect that the number of tracks recorded in each grid box is proportional to its effective cross-sectional width, which varies according to the orientation of the tracks (Taylor 1986). This causes grid-dependent biases, which cannot be

satisfactorily corrected. In this scheme, the problems of having to define cross-sections and to avoid multiple counts are obviated by taking account of the fact that, for a given density, the flux of cyclones will be proportional to their speeds (or velocity components). Flux is therefore found by weighting the frequency counts by the sampled velocity. As before, the summations are normalised for area and number of sampling periods but, owing to the velocity weighting, are effectively scaled only linearly for distance.

#### Optimisation of tracking parameters

The decisions of the tracking program are guided by a number of governing parameters and a set of prediction velocities purporting to represent the zonal climatological mean velocities ( $v_{a1}(\phi)$ ). Initially, an arbitrary but realistic set of figures was chosen and the cyclones were tracked for ten days. By adjusting the parameters separately and comparing the plotted tracks with those arrived at subjectively from an examination of the successive daily charts, such as Fig.6, a usable (but not necessarily optimum) set of constants and velocities was arrived at.

Experience showed that, while in the majority of cases the tracking program was making the 'correct' decisions, there was always a small number of apparent discrepancies which could not be eliminated, whatever adjustments might be made to the controlling constants. Although cyclones from both the WMC numerical analyses and from the model data suffered from this problem, the former were found to behave very much more erratically, even though the analyses were available at 12-hourly intervals. Whether this was more a problem of areal coverage (which does not arise with model output) and data quality or rather a consequence of the complexity of atmospheric processes, which are simplified and truncated in a computer simulation, is not clear. In any event, it was decided, for the time being, to apply the scheme to the GCM cyclones which appeared to be tracking in the desired manner most of the time.

A more objective set of prediction velocities might be obtained from the averaged velocities resulting from the tracking of cyclones over long series of data. Since the tracked movement of a cyclone is determined not only by the average velocity forcing but also by the displacement of the system during the previous time interval and the availability of new cyclone positions, one would expect the tracked velocities to approximate the climatology of the data set more closely than the original prediction velocities and therefore to be suitable for use as an improved set of prediction velocities. With repeated cycling one might expect these 'climatological' velocities to converge to stable values. An example of this refinement is illustrated in Table 1. The convergence is rather



**Table 1.** Optimisation of prediction velocities (units  $\text{m s}^{-1}$ ).

Lat. zone (°S)	First guess		First refinement		Second refinement		Third refinement	
	u	v	u	v	u	v	u	v
15-20	-0.5	-1.2	-0.4	-1.3	-0.4	-1.3	-0.4	-1.3
20-25	0.3	-1.7	0.9	-1.7	0.9	-1.7	0.9	-1.7
25-30	5.0	-2.9	4.4	-2.2	4.4	-2.1	4.4	-2.1
30-35	8.9	-3.3	7.9	-2.9	7.9	-2.8	7.9	-2.9
35-40	9.1	-3.1	9.4	-2.8	9.6	-2.9	9.6	-2.9
40-45	8.4	-2.7	10.2	-2.6	10.6	-2.6	10.7	-2.6
45-50	8.7	-2.8	10.3	-3.0	10.8	-2.9	11.0	-2.9
50-55	8.6	-2.8	9.3	-2.0	9.5	-2.0	9.6	-2.0
55-60	7.7	-1.9	7.6	-1.6	7.7	-1.6	7.7	-1.6
60-65	4.3	-1.2	4.6	-1.3	4.8	-1.3	4.8	-1.4
65-70	2.2	-0.4	2.6	-1.1	2.7	-1.2	2.7	-1.2
70-75	-0.1	-0.2	1.5	-1.2	1.7	-1.2	1.7	-1.2
75-80	3.7	-0.1	0.9	-1.2	0.8	-1.1	0.7	-1.2
80-85	1.8	-0.3	0.9	-0.2	0.7	0.0	0.6	-0.1
85-90	1.6	-0.8	1.8	-0.6	1.7	-0.3	1.3	-0.3

slow (the sensitivity of resulting velocities to prediction velocities being of the order of 30 per cent) so a few passes through the data are necessary. Also some manual intervention may be appropriate at high latitudes where the numbers of lows are small. The procedure is routinely carried out each time cyclones from a new data set are tracked.

Some of the control parameters are also amenable to similar improvement, but the results have been only used for guidance. The optimum weighting used in the pressure prediction was found by minimising the variance of the 'error',  $\delta p = p_{new}(t+\delta t) - p_{cs}(t+\delta t)$ , with respect to  $w_p$ . An estimate of the movement weighting factor,  $w_M$ , was obtained in a similar way. The weighting factors were found to be latitude dependent, however values representative of the mid-latitude range were found to be consistent with those chosen subjectively.

## Performance of the tracking scheme

### Tracking at short time intervals

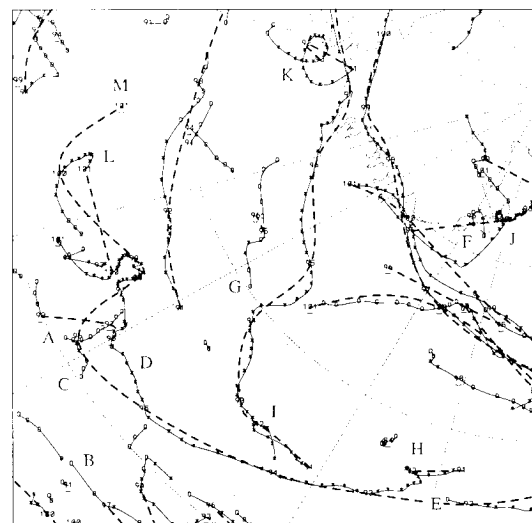
In order to gain a better insight into the 'true behaviour' of the modelled depressions, the 21-wave July simulation was repeated over a ten-day period so that MSL pressure fields might be extracted at three-hourly intervals. Cyclones were found by the scheme (using a relaxed concavity criterion) and tracked using these data. Since no system travels more than about 2 deg. lat. in this time, there would be almost no uncertainty in the association of successive positions. The three-hourly tracked positions of cyclones in a sector of the South Pacific are compared with the results of 24-hourly tracking in Fig. 10. A number of interesting aspects of the behaviour of the simulation may be noted.

The three-hourly positions of both closed and open depressions are seen to progress in a fairly

regular and consistent manner. This was an unexpected bonus, which helped to justify the method of analysing open depressions and the use of fractional grid-point positions for locating lows.

Open depressions were interspersed amongst closed depressions along some tracks. One is inclined to regard these as instances of the weakening of a system followed by its reintensification. On tracks composed entirely of open depressions the decay of  $\nabla^2 p$  value beyond the threshold value may disrupt it entirely, as appears to have happened on track A in Fig. 10. Variations in the

**Fig. 10** Tracks of cyclones for ten days over a sector of the South Pacific from positions at three-hour intervals (solid curves). The numbered daily positions are also connected by tracks (dashed) computed at 24-hour intervals. Open depressions are underscored (daily positions) or marked by circles (intermediate times).



intensity of systems are, to some extent, an artifact of the interpolation, which slightly enhances depressions when they naturally fall close to grid boundaries. This property probably accounts for the uneven progression of some marginal systems, as observed in track B.

That open depressions do assist the tracking is demonstrated in the case of a subsidiary low, C, which formed to the north of a mature cyclone, D, and actually overtook it in intensity for a few hours before disappearing, but maintained a separate identity throughout. In some situations, open depressions have heralded the genesis of cyclones at an earlier stage and marked their demise at a later stage than would have been possible without them (E-H). Whether such positions need be retained for the statistical summations may be debated. Not uncommonly these outlying positions occur close to continuing systems, which may at the same time suddenly change direction (E,G). The scheme has been programed to treat cyclogenesis and cyclolysis as the end points of a linear evolution, but a more appropriate model for many occasions may be one of division and merging.

Several examples are observable where the tracking at 24-hour intervals was not able to accommodate sudden changes in the speed or direction of movement of a system (C,E,L,M), especially where progress had become retrograde in latitudes of high average eastward motion. Many retrograde loops are evident (H-L), most of them curving in a cyclonic sense.

The weighting factors,  $w_M$  and  $w_P$ , were calculated from tracking runs made at 3, 6, 12 and 24-hour intervals. The values of  $w_P$  were found to conform with the exponential decay assumption quite well, but the figures for  $w_M$  did not follow any clear trend. This failure may be related to the tendency of the interpolation to select preferred positions within the grid squares.

#### Improvement of cyclone distributions and tracking behaviour

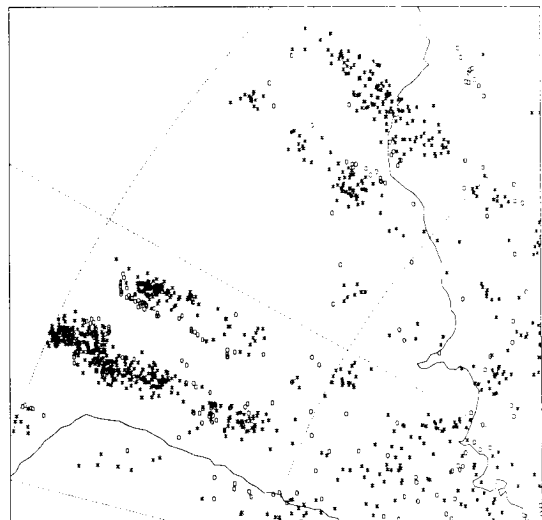
The problems encountered in tracking cyclones are partly a consequence of using data spaced at 24-hour intervals, during which time many systems travel distances comparable with their separations. The restrictions which must then be imposed upon the radii of search make it difficult for the scheme to anticipate sudden changes of velocity which real systems often undergo. Examples of such sudden changes in speed and direction may be seen in the 12-hourly positions tracked by Neal (1972) and Lamond (1972) from charts of the GARP Basic Data Set Analysis Project (November 1969 and June 1970). We believe that the statistical basis of the tracking program is consistent with the performance of its intended task within the desirable constraints of speed, simplicity, and a minimum of data input, but acknowledge that the incorporation of some type

of simple dynamical prognostic model might improve the prediction of new positions.

The use of short time intervals would all but eliminate errors of tracking by effectively using the model to predict cyclone movements. This approach has been contemplated, but the benefits of using more frequent data need to be balanced against the extra computer time required to extract the required fields from the model data (when available) and apply the tracking scheme to them. Such an intensive approach may be appropriate for case studies of cyclone evolution, where a faithful rendering of the system histories is important. An attempt was made to simulate pressure fields at intermediate times using (cubic spline) time interpolation of the daily data, but the depressions generated by this technique did not maintain a continuous identity.

Uncertainty in the prediction of displacements is not the only source of error in tracking cyclone movements. Defects in the numbers and positions of cyclones analysed from the data fields and in their consistency from day to day can also lead to tracking errors and biases in the statistics. A problem particularly apparent with the 21-wave model data was the large number of systems, both open and closed, found within or to the north of the subtropical high pressure belt. Some of these centres may have been the modelled equivalents of real quasi-stationary depressions, but the high densities of pressure minima (over land and sea) exposed the tracking program to a tendency to link them together into moving systems, and at latitudes where large numbers of migratory systems were not expected. The innovation of a minimum concavity criterion has substantially eliminated this problem and seems at the same

Fig. 11 Positions of cyclones (including ephemeral systems) over South America in the 21-wave January simulation.



time to have resulted in an improvement in the tracking of mid-latitude cyclones.

Some spurious features of the cyclone distribution are illustrated in Fig. 11, which shows the positions of cyclones over South America during the 600 days of the January simulation. A high concentration of lows has persisted over northern Chile even after considerable diminution by the concavity criterion. This is believed to be an artifact of the reduction of surface pressures over the Andes to MSL. The low centres are preferentially aligned along the meridians of the  $5.6^\circ$  longitude  $\times$   $3.3^\circ$  latitude (Gaussian) grid on which the MSL pressures are mapped before being recast on a PS grid. The effect is most noticeable at low latitudes, where the meridians are widely spaced and background pressure gradients are weak.

Local variations in cyclone numbers from day to day, beyond those attributable to the actual birth and death of cyclones, were another nuisance. They not only exaggerated frequencies of cyclogenesis and cyclolysis but inevitably resulted in tracking errors. In real analyses the appearance and disappearance of lows may be due to uneven data coverage; in the case of model data it is likely that spectral truncation may be preventing the resolution of mesoscale thermal contrasts, which help to maintain the strength and identity of individual vortices. The problem of varying cyclone numbers has been alleviated by the inclusion of open depressions, which help to maintain the continuity of many tracks, but a residual bias no doubt exists.

#### Sensitivity of cyclone statistics to the governing parameters

For the purpose of analysing the synoptic behaviour of long series of data, it may be that the effects of tracking errors will tend to cancel out in

the mean statistics. If this is the case one may expect the averages to be comparatively insensitive to the exact choice of parameters. To test this assumption we tracked July cyclones for a 60-day period, using parameters and velocities which had been found suitable over longer periods, and obtained averages in  $10^\circ$  latitude bands. This was repeated a number of times using in each case a modified value of a single parameter. The alterations involved the modification of several tracking parameters ( $r_c$ ,  $P_{open}$ ,  $P_{new}$ , and  $k_{rp}$ ), the relaxation of the concavity criterion, the imposition of a 72-hour minimum lifetime, and the augmentation of the  $u$  component of the prediction velocity ( $u_{pred}$ ) by  $2 \text{ m s}^{-1}$  at all latitudes. Averages of several quantities in selected latitude bands are presented in Table 2.

It will be seen that alterations in the tracking parameters have brought about moderate changes in cyclone frequencies in the expected directions but have not affected velocities. For instance, a widening of the radius of search ( $r_c$ ) or a milder discrimination against open depressions (greater  $P_{open}$ ) favours the continuity of tracks, thereby increasing cyclone densities (since fewer ephemeral systems are rejected) while diminishing the creation of new cyclones. On the other hand, the increased prediction velocities have affected the velocity statistics but not the frequencies. It thus appears that the independent tuning of velocities is justified. Neither tracking parameters nor prediction velocities have resulted in perceptible changes to the central pressures.

The largest sensitivities were associated with the concavity test (as normally done to remove insignificant depressions) and with a longer minimum lifespan criterion. Both had the effect of severely curtailing total cyclone frequencies and of lowering average central pressures.

Table 2. Sensitivity of zonal averages to variation of parameters.

Parameter alteration	(No change)	$r_c = 1.5^\circ$	$P_{open} = 0.8$	$P_{new} = 1.0$	$k_{rp} = 1.2$ hPa/°	Concav. test = no	Life-span = 72 h	$u_{pred} = \bar{u} + 2$ $\text{m s}^{-1}$	
(control value)		(1.25)	(0.6)	(0.8)	(1.4)	(yes)	(24)	( $\bar{u}$ )	
Cyclo- genesis (nos)	20–40°S	42	44	46	46	42	121	25	42
	40–60°S	106	100	107	111	107	118	51	106
	60–80°S	50	39	50	54	52	59	34	48
Cyclone density (no./deg. <sup>2</sup> )	20–30°S	0.13	0.13	0.13	0.13	0.13	0.78	0.09	0.13
	40–50°S	1.33	1.38	1.37	1.36	1.29	1.67	1.21	1.33
	60–70°S	1.79	2.01	1.90	1.83	1.68	2.09	1.63	1.78
Eastward velocity ( $\text{m s}^{-1}$ )	20–30°S	4.0	4.3	4.3	4.0	4.0	4.3	5.0	4.2
	40–50°S	10.4	10.5	10.4	10.3	10.1	10.3	10.4	10.8
	60–70°S	6.2	6.5	6.4	6.3	6.2	6.5	6.4	7.3
Central pressure (hPa)	20–30°S	1007.7	1007.6	1007.6	1007.7	1007.7	1013.1	1006.9	1007.6
	40–50°S	990.4	990.5	990.6	990.3	990.3	992.9	989.7	990.1
	60–70°S	977.0	977.5	997.6	977.2	977.1	978.7	976.7	977.3

## Concluding remarks

The scheme described herein is believed to have substantially achieved the aim of providing an efficient and much needed tool for the study of extratropical cyclone climatologies. The accuracy of the output has been assessed with reference to isobaric charts and, more objectively, by comparisons with plots of cyclone positions spaced at short time intervals. The cyclone finding and statistical routines performed quite satisfactorily but a number of difficulties were experienced in tracking the model cyclones reliably from daily data. These were compounded by a spuriously high incidence of lows in subtropical regions. Modifications to the finding program to enable the identification of open depressions and the exclusion of insignificant depressions using a concavity criterion were found to result in a rather more credible set of cyclone tracks and statistics.

The programs have been tested and found to operate reliably with the 15 and 21-wave model data and have been used to investigate the cyclone climatology of the 21-wave simulations: the results of this study will be reported in Part II. Their application to a parallel study of historical data and to the analysis of a number of model sensitivity studies is also contemplated.

The scheme as it stands has been tailored to work with SH mid-latitude cyclones on a PS grid of around 400 km resolution, but it could equally well be employed for finding and tracking the maxima or minima of any atmospheric property at MSL or at any upper level, and with suitable modification, on any global or regional grid. Some of these difficulties encountered were peculiar to the data, the time interval between analyses, and grid resolution used; in other applications of the scheme they might evaporate or be different.

The three stages of the scheme have been designed to operate in tandem but there is no reason why they should not be used independently. For instance, the positions and central pressures transcribed from operational charts could be introduced at the tracking stage, or data from published tracks could be analysed directly by the statistical program. Another possibility would be to apply the scheme to following the movements and pressure tendencies of individual storms. This would be helpful in the analysis of errors in model forecasts or (when used on a fine mesh and with data at frequent intervals) in investigations of the evolution of deep depressions and of the radial and vertical distribution of atmospheric properties around them.

## References

- Bell, G.D. and Bosart, L.F. 1989. A 15-year Climatology of Northern Hemisphere 500 mb Closed Cyclone and Anticyclone Centres. *Mon. Weath. Rev.*, 117, 2142-63.
- Carleton, A.M. 1979. A Synoptic Climatology of Satellite-Observed Extratropical Cyclone Activity for the Southern Hemisphere Winter. *Arch. Met. Geophys. Bioklim.*, B, 27, 265-79.
- Grotjahn, R. 1900. Feature-Based Predictability of 500 hpa Height in the Australia-New Zealand Region. *Meteorol. Atmos. Phys.*, 42, 57-67.
- Guymer, L.B. 1978. Operational application of satellite imagery to synoptic analysis in the Southern Hemisphere. *Tech. Rep. No.29*, Bur. Met., Australia.
- Guymer, L.B. 1986. Procedures and Concepts used in Southern Hemisphere Analyses at WMC Melbourne. *Second International Conference on Southern Hemisphere Meteorology, Dec. 1986*, Amer. Met. Soc., 10-16.
- Hayden, B.P. 1981. Cyclone Occurrence Mapping: Equal Area or Raw Frequencies? *Mon. Weath. Rev.*, 109, 168-72.
- Kep, S.L. 1984. A Climatology of Cyclogenesis, Cyclone Tracks and Cyclolysis in the Southern Hemisphere for the period 1972-81. *Publication No. 25*, Department of Meteorology, University of Melbourne.
- Klein, W.H. 1957. Principal tracks and mean frequencies of cyclones and anticyclones in the Northern Hemisphere. *Rev. Pap. No. 40*, U.S. Weather Bureau, Washington D.C., 60 pp.
- Lambert, S.J. 1988. A Cyclone Climatology of the Canadian Climate Centre General Circulation Model. *J. Climate*, 1, 109-115.
- Lamond, M.H. 1972. Cyclone Tracks in the High Latitudes in November 1969 and June 1970. *Aust. Met. Mag.*, 20, 248-58.
- Le Marshall, J.F. and Kelly, G.A.M. 1981. A January and July climatology of the Southern Hemisphere based on daily numerical analyses 1973-77. *Aust. Met. Mag.*, 29, 115-23.
- Le Treut, H. and Kalnay, E. 1990. Comparison of observed and simulated cyclone frequency distribution as determined by an objective method. *Atmosfera*, 3, 57-71.
- Murray, R.J. and Simmonds, I. 1991. A numerical scheme for tracking cyclone centres from digital data. Part II: application to January and July general circulation model simulations. *Aust. Met. Mag.*, 39, 167-80.
- Neal, A.B. 1972. MSL Cyclones and Anticyclones in November 1969 and June 1970. *Aust. Met. Mag.*, 20, 217-30.
- Reitan, C.H. 1974. Frequencies of Cyclones and Cyclogenesis for North America, 1951-1970. *Mon. Weath. Rev.*, 102, 861-8.
- Rice, J. 1982. The Derivation of Computer-based Synoptic Climatology of Southern Hemisphere Extratropical Cyclones. Honours Thesis, Department of Meteorology, University of Melbourne.
- Simmonds, I. 1985. Analysis of the 'spinup' of a general circulation model. *J. Geophys. Res.*, 90, 5637-60.
- Streten, N.A. and Troup, A.J. 1973. A synoptic climatology of satellite observed cloud vortices over the Southern Hemisphere. *Q. Jl R. met. Soc.*, 99, 56-72.
- Taljaard, J.J. 1967. Development, Distribution, and Movement of Cyclones and Anticyclones in the Southern Hemisphere during the IGY. *Jnl appl. Met.*, 6, 973-87.
- Taylor, K.E. 1986. An Analysis of the Biases in Traditional Cyclone Frequency Maps. *Mon. Weath. Rev.*, 114, 1481-90.
- Whittaker, L.M. and Horn, L.H. 1982. *Atlas of Northern Hemisphere Extratropical Cyclone Activity, 1958-1977*. University of Wisconsin, 65 pp.
- Williamson, D.L. 1981. Storm track representation and verification. *Tellus*, 33, 513-30.
- Zishka, K.M. and Smith, P.J. 1980. The Climatology of Cyclones and Anticyclones over North America and Surrounding Ocean Environs for January and July, 1950-77. *Mon. Weath. Rev.*, 108, 387-401.